Table V—Incremental Constant Evaluating Effect of Molecular Modification of Side Chain of Cholesterol on Permeability and Partition Coefficients of Desmosterol and β-Sitosterol

Parameter	Incremental Constant	
	Desmosterol	β-Sitosterol
$K_{sterol}/K_{cholesterol}$	3.26	0.65
$P_{sterol}/P_{cholesterol}$	3.0	0.53

permeability coefficients by a factor of two. The interpretation of these molecular modifications of cholesterol is unclear. It is apparent that the expectation of increased partition coefficient with decreasing polarity of the solute is not found here.

REFERENCES

(1) J. S. Turi, N. F. H. Ho, W. I. Higuchi, and C. Shipman, Jr., *J. Pharm Sci.*, **64**, 622(1975).

(2) *Ibid.*, **61**, 1618(1972).

(3) G. H. Rothblatt and C. H. Burns, *J. Lipid Res.*, **12**, 653(1971).

(4) N. F. H. Ho and W. I. Higuchi, *J. Pharm. Sci.*, **60**, 537(1971).

(5) K. R. Vora, W. I. Higuchi, and N. F. H. Ho, *ibid.*, **61**, 1785(1972).

(6) N. F. H. Ho, "Abstracts of Academy of Pharmaceutical Sciences," APhA Academy of Pharmaceutical Sciences, Washington, DC 20037, 1972, p. 112.

ACKNOWLEDGMENTS AND ADDRESSES

Received February 13, 1974, from **Pharmacy Research, The Upjohn Company, Kalamazoo, MI 49001*, the ‡*College of Pharmacy, University of Michigan, Ann Arbor, MI 48104*, and the §*Dental Research Institute, Department of Oral Biology, School of Dentistry and the Department of Microbiology, School of Medicine, University of Michigan, Ann Arbor, MI 48104*

Accepted for publication July 19, 1974.

ˣ To whom inquiries should be directed.

Systems Approach to Study of Solute Transport across Membranes Using Suspension Cultures of Mammalian Cells V: Uptake and Release Kinetics of Cardiac Glycosides by Burkitt Lymphoma Cells

J. S. TURI *ˣ, N. F. H. HO ‡, W. I. HIGUCHI ‡, and C. SHIPMAN, Jr. §

Abstract □ Mass transport studies with three cardiac glycosides in the Burkitt lymphoma cell system have provided significant examples of the factorization and quantification of the influences of serum–drug binding, membrane–drug binding, cell interior binding, and intrinsic membrane permeability upon the uptake and release kinetics of drugs in living cell systems. All of the data from the glycosides are in agreement with the general physical model involving the rapid equilibration of the solute within the cell after permeation through the rate-determining plasma membrane barrier. The transport of digitoxin was influenced by membrane and serum binding and that of digoxin was influenced by membrane binding. There was no binding of ouabain to the plasma membrane and serum. The variables in the uptake and release kinetic studies at pH 7.3 included the use of viable and heat-inactivated cells, fetal bovine serum levels, and temperature.

Keyphrases □ Membrane diffusion—systems approach to drug transport, uptake and release of cardiac glycosides by Burkitt lymphoma cells, influence of serum–drug binding, membrane–drug binding, cell interior binding, and intrinsic membrane permeability □ Drug transport—uptake and release kinetics, cardiac glycosides, Burkitt lymphoma cells, influence of serum–drug binding, membrane–drug binding, cell interior binding, and intrinsic membrane permeability □ Mammalian cells, suspension culture—uptake and release of cardiac glycosides, systems approach to study of drug transport across membranes □ Cardiac glycosides—kinetics of uptake and release by Burkitt lymphoma cells, systems approach to drug transport

The lack of a mechanistic and quantitative understanding of the kinetics of drug transport to the receptor site has impeded the quantitative approach to drug design. Nearly all previous studies in the field have been of a rather descriptive nature; it has been difficult to separate, for example, the driving force factors from the kinetic factors in describing the transport and the bioavailability of drugs at the site of action from a physical–chemical standpoint.

Existing evidences indicate that one cannot always rely solely on oil–water partition coefficients, blood levels of drugs, or rates of intestinal transport as true indications of drug availability at the site of drug action. It is believed that the developed physical models and experimental techniques will give more insight into drug availability, especially at the receptor site. The concepts put forth here can be valuable in assessing molecular modifications of drugs. This study illustrates that collaborative research among pharmacokineticists, medicinal chemists, and experts in mass transport across biological membranes can be very valuable in assessing drug availability.

This paper describes the mass transport of ouabain, digoxin, and digitoxin in suspension cultures of an established cell line. This study evolved from the development of various biophysical models (1, 2) and the accompanying experimental systems and techniques. Its significance lies not only in the important implication it may have on the understanding of the

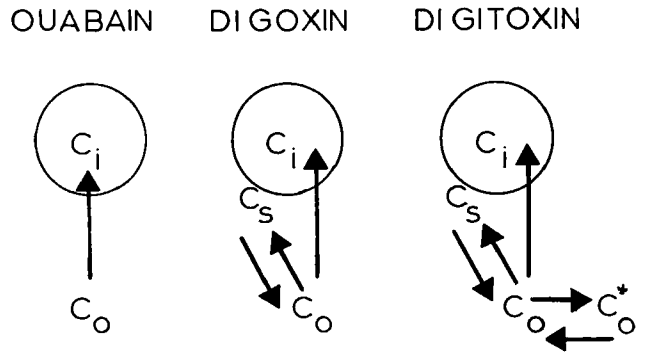

Figure 1—*Schematic physical model of the uptake transport of the cardiac glycosides. The term C_0 is the concentration of drug outside of the cell, C_i is the concentration inside of the cell, C_s is the concentration adsorbed on the plasma membrane surface, and C_0* is the concentration of serum-bound drug.*

pharmacokinetics of the cardiac glycosides in humans but also, from the standpoint of methodology, in providing examples of the factorization and quantification of the influences of serum–drug binding, membrane–drug binding, cell interior binding, and the intrinsic membrane permeability upon the uptake and release kinetics of drugs in living cell systems.

EXPERIMENTAL

Materials and Methods—The materials, methods, and procedures in the cultivation and preparation of Burkitt lymphoma cells were described previously (3). The uptake and release kinetic experiments of radiolabeled ouabain-^{3}H, digoxin-^{3}H, and digitoxin-^{3}H cardiac glycosides[1] were conducted in a manner identical to that employed previously for cholesterol, desmosterol, and β-sitosterol (3, 4).

In the uptake studies, the drug was added to 100-ml water-jacketed spinner flasks[2] containing about 4×10^8 viable cells in 100 ml of culture medium at pH 7.3, under isoosmotic and sterile conditions. The suspending medium contained modified McCoys 5A, basal medium Eagle, balanced salt solution, penicillin G (50 units/ml) and amphotericin B (1 μg/100 ml). The variables included fetal bovine serum concentrations, drug concentrations, and temperature.

To follow changes in drug concentration with time, 5-ml samples

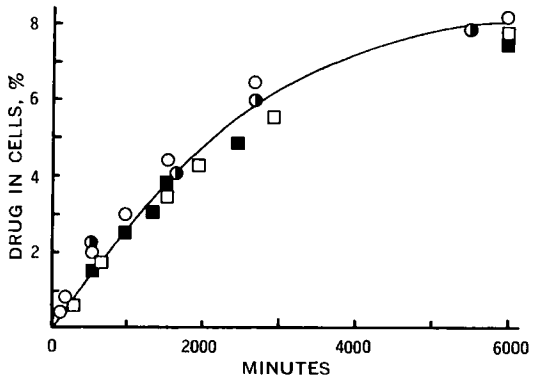

Figure 2—*Uptake of ouabain at 26° by viable and nonviable Burkitt cells at various fetal bovine serum concentrations. The solid curve represents the best theoretical fit of the model by nonlinear regression analysis. Key: ○, 0%; □, 15%; ■, 30%; and ◑, 0% (heat-inactivated cells).*

were centrifuged in thrombocytocrit tubes at 5000×g for 10 min and both the cell and extracellular fractions were assayed by liquid scintillation counting. Total cell numbers in the samples were determined[3].

To study the release kinetics, the static equilibration technique was used to load the cells with the radiolabeled drug. Viable cells in culture suspension were allowed to mix with the drug at 26° for at least 48 hr. Thereafter, the equilibrated cells were washed and resuspended in fresh medium and the release studies followed the sampling procedure for the uptake studies.

Uptake and release kinetic studies were performed at 26, 30, and 33°. Although somewhat removed from the physiological temperature of 37°, these temperatures were chosen to prevent cell division during the experiments and yet sustain a level of metabolic activity.

In some instances, nonviable cells were utilized. These were cells in which the cellular enzymes were inactivated by heat at 50° for 30 min. Viability was assessed by the erythrocin B dye exclusion method. When viable cells were used, at least 90% of the cell population remained viable after 24 hr and 50% was viable after 48 hr. As indicated by the particle counter and multichannel pulse height analyzer, the cell population and the quite narrow size distribution at the beginning and end of the experiments were essentially superimposable.

The methods and procedures of these kinds of experiments have already been shown to be precise, accurate, and reproducible. There was less than 2% drug entrapment in the centrifuged cell plug, well within the experimental error. These experimental techniques are highly quantitative when the transport rate is essentially membrane controlled (*i.e.*, low permeability coefficient), as was shown in the sterol studies and in this present study. Refined techniques are being developed for situations when the transport rate becomes less membrane controlled and more controlled by the stagnant aqueous layer about the cell.

To evaluate drug–serum binding, the experimental dialysis setup used two spinner flasks of 150-ml capacity each and a dialysis membrane placed at the flanged connection. The surface area of the exposed membrane was 5.07 cm^2 and had a pore size of 24 Å.

Uptake and Release Kinetics of Ouabain—*Theoretical*—The kinetics of cell uptake and release of ouabain can be explained by Model 1, the simplest of the various models previously derived (2). Figure 1 is a schematic illustration of the passive transport of unbound drug molecules across the rate-determining plasma membrane with rapid distribution of the drug in the heterogeneous cell interior. There is no binding of the drug to the surface of the cell nor to the serum and other components comprising the external medium of the culture suspension.

The uptake transport function of this model, UF_1, is:

$$UF_1 = -\frac{a}{180B} \ln\left[1 - \frac{B}{A}C_i\right] = Pt \qquad \text{(Eq. 1)}$$

$$A = T/V_0 \qquad \text{(Eq. 2)}$$

$$B = \frac{nV_i}{V_0} + \frac{1}{K} \qquad \text{(Eq. 3)}$$

where a is the radius of the cell, n is the number of cells, V_i is the volume of a cell, V_0 is the volume of the external aqueous phase, T is the total amount of drug in the system, C_i is the concentration of drug in a cell, K is the intrinsic partition coefficient, P is the intrinsic permeability coefficient of the plasma membrane, and t is time. The initial boundary condition is $C_i(0) = 0$.

A plot of UF_1 *versus* t in minutes is linear with a slope equal to P in units of centimeters per second. The permeability coefficient can also be found by nonlinear regression analysis of the nonlinear form of Eq. 1. In both cases, the intrinsic partition coefficient must be first determined.

For initial rates, Eq. 1 reduces to:

$$C_i = \frac{3PT}{aV_0}t \qquad \text{(Eq. 4)}$$

[1] New England Nuclear Corp., Boston, Mass.
[2] Bellco Glass, Inc., Vineland, N.J.
[3] Coulter counter model A.

Table I—Permeability and Partition Coefficients of Ouabain at Various Temperatures and Fetal Bovine Serum Concentrations from Uptake Kinetics[a]

Fetal Bovine Serum, %	Intrinsic Partition Coefficient K			Intrinsic Permeability Coefficient P, cm/sec $\times 10^8$		
	26°	30°	33°	26°	30°	33°
0	12.2 ± 0.8	16.0 ± 1.0	20.7 ± 3.1	2.08 ± 0.43	4.18 ± 0.1	7.69 ± 0.84
0[b]	14.0	—	—	2.38	—	—
5	—	—	16.5 ± 0.7	—	—	4.78 ± 0.03
15	13.0 ± 1.4	14.0 ± 1.7	15.0 ± 2.8	1.73 ± 0.11	2.76 ± 0.12	4.38 ± 0.04
15[c]	—	16.0 ± 1.4	—	—	2.49 ± 0.1	—
30	11.3 ± 1.5	—	16.0 ± 1.0	1.58 ± 1.53	—	4.35 ± 0.14

[a] The values of K were found from the equilibrium data according to Eq. 5, and the values of P were found from nonlinear regression analysis of the model. [b] Heat-inactivated Burkitt lymphoma cells used here; viable cells in culture suspension were utilized in all other studies. [c] Partition and permeability coefficients were calculated from release kinetics from viable cells at 30° using 15% fetal bovine serum.

Thus, the intrinsic permeability coefficient can be readily obtained from the initial slope of a C_i *versus* t plot.

The intrinsic partition coefficient can be experimentally found from the equilibrium condition, *i.e.*, when $(dC_i/dt)_{t=\infty} = 0$; thus:

$$K = \frac{C_{i,\infty}}{C_{0,\infty}} \qquad \text{(Eq. 5)}$$

where $C_{0,\infty}$ and $C_{i,\infty}$ are the concentrations of drug in the external medium and cell at equilibrium, respectively.

The release transport function, RF_1, is expressed by:

$$RF_1 = \frac{a}{180B} \ln\left[\frac{BC_i - A}{BC_i(0) - A}\right] = -Pt \qquad \text{(Eq. 6)}$$

The initial boundary condition is $C_i = C_i(0)$.

Analysis of Results—Figure 2 shows the uptake kinetics of ouabain by viable cells at three fetal bovine serum concentrations at 26° and by heat-inactivated cells with no fetal bovine serum. The partition coefficients are found from the plateau region of these plots. As illustrated in Fig. 3, the application of theory (Eq. 1) to the data yields the predicted linear relationship of the uptake transport function, UF_1, *versus* time.

The permeability coefficients, found by the best theoretical fit of the data in Fig. 2 and linear regression of the plot in Fig. 3, were not significantly different from each other. Table I summarizes the phenomenological transport constants of ouabain with respect to the Burkitt cell under varying conditions of temperature, cell viability, and fetal bovine serum concentration.

The following observations and comments can be made:

1. At any specific temperature, there are no significant differences between the permeability coefficient and partition coefficient themselves at the 15 and 30% fetal bovine serum levels. This is an indication that there is no occurrence of ouabain–serum binding, which will be further corroborated by dialysis experiments in the next section. However, these coefficients appear to be larger at 0% fetal bovine serum with respect to those at 15 and 30% fetal bovine serum, and the deviation tends to increase with increasing temperature. A similar observation was noted with the transport of cholesterol, desmosterol, and β-sitosterol at 26° with the Burkitt cells (4) and unpublished findings of digitoxin with red blood cells at 0% fetal bovine serum in these laboratories. There apparently is some degree of alteration of the plasma membrane in the absence of serum and the change is more apparent at higher temperatures.

2. There is a temperature dependence in the permeability coefficients. After applying the Arrhenius-type relationship of the permeability coefficients to temperature, the heat of activation is found to be about 24 kcal/mole. The temperature dependence of the partition coefficients is very small.

Evaluation of Serum Binding by Dialysis—According to the setup of the dialysis experiments, the rate of dialysis is:

$$\frac{dC_r}{dt} = \frac{A_m P_{em}}{V_r}(C_d - C_r) \qquad \text{(Eq. 7)}$$

and, with $C_r(0) = 0$, the solution is described in the following manner:

$$DF = -\frac{V_r}{120A_m} \ln\left(1 - \frac{2C_r}{T}\right) = P_{em}t \qquad \text{(Eq. 8)}$$

where C_d and C_r are the total concentrations of the drug in the donor and receiving compartments of equal volume, respectively; V_r is the volume of solution of the receiving compartment; A_m is the effective surface area of the dialysis membrane; P_{em} is the effective permeability coefficient of the membrane; t is the time; and DF is the dialysis function.

A plot of DF *versus* t in minutes gives a straight line with a slope of P_{em} in centimeters per second. The long times required to reach equilibrium are due to both the small effective surface area-to-volume ratio of 1:40 and also the pore size of the dialysis membrane of 24 Å diameter as compared to the molecular size of the cardiac glycosides.

The results in Fig. 4 clearly show that there is no serum binding with ouabain as well as digoxin. The dialysis profiles are identical between both of these cardiac glycosides at zero and 30% fetal bovine serum at 26° and pH 7.3. However, digitoxin does adsorb to

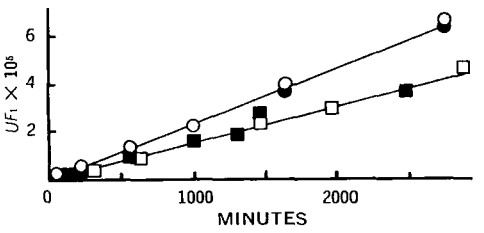

Figure 3—*Profiles of uptake kinetics of ouabain at various fetal bovine serum concentrations at 26° according to the linear predictions of Eq. 1. Solid lines are least-squares lines. Key: ○, 0%; □, 15%; ■, 30%; and ●, 0% (heat-inactivated cells). Faster uptake kinetics at 0% fetal bovine serum are attributed to altered integrity of the plasma membrane when no serum is present.*

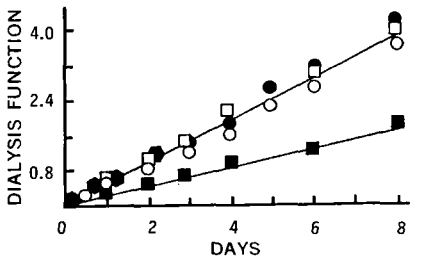

Figure 4—*Kinetics of dialysis of ouabain, digoxin, and digitoxin in the presence of fetal bovine serum at 26°. The dialysis function is defined by Eq. 8. Key: □, digitoxin–0%; ■, digitoxin–30%; ○, digoxin–0%; ●, digoxin–30%; and ●, ouabain–30%. Ouabain with no fetal bovine serum was similar to ouabain–30% fetal bovine serum. Taken together, the data show that ouabain and digoxin do not bind to fetal bovine serum while digitoxin does.*

Table II—Evaluation of Plasma Membrane–Digoxin Equilibrium Binding Constant, K_{bm}, under Varying Conditions of Initial Drug Concentrations, Serum Levels, and Temperature from Uptake Kinetic Studies[a]

Temperature	Fetal Bovine Serum, %	Initial Amount Adsorbed per 10^6 Cells, dpm	Total Amount of Drug in 5 ml Suspension, dpm	K_{bm}
26°	0	210	3.28×10^5	1.82
	15	228	3.22×10^5	1.96
33°	0	295	6.98×10^5	1.20
	5	290	6.57×10^5	1.24
	15	285	6.25×10^5	1.28
	30	294	7.05×10^5	1.17

[a] The K_{bm} is 1.89 at 26° and 1.22 at 33°.

fetal bovine serum. Similar findings were reported previously (1).

Uptake and Release Kinetics of Digoxin—*Theoretical*—The kinetics of cell uptake and release of digoxin can be appropriately described by Model 4 (2), in which the unbound drug permeates passively across the plasma membrane and distributes rapidly in the heterogeneous interior of the cell (Fig. 1). However, there is an instantaneous, reversible binding of the drug molecules to the external side of the plasma membrane. The membrane-bound drug is in equilibrium with the free drug in the external medium; there is no significant binding of the drug to the serum in the medium.

According to the model, the uptake transport function is given by:

$$UF_4 = -\frac{a(1 + K_{bm}E)}{180G} \ln\left[\frac{F - GC_c}{F - GC_c(0)}\right] = Pt \quad \text{(Eq. 9)}$$

$$E = \frac{nV_i}{V_0} \quad \text{(Eq. 10)}$$

$$F = \left(1 + \frac{K_{bm}}{K}\right)\frac{T}{V_0} \quad \text{(Eq. 11)}$$

$$G = \left(1 + \frac{K_{bm}}{K}\right)\frac{nV_i}{V_0} + \frac{1}{K} \quad \text{(Eq. 12)}$$

where K_{bm} is the plasma membrane–drug equilibrium adsorption constant; K and P are the intrinsic partition and permeability coefficients, respectively; C_c is the concentration of drug in the cell, which includes the drug within the cell and the drug adsorbed to the external surface of the plasma membrane; and $C_c(0)$ is the cell concentration at zero time and is equal to the initial surface-adsorbed drug concentration. It follows that the intrinsic permeability coefficient can be obtained from the application of the linear or nonlinear form of Eq. 9.

The membrane–drug equilibrium adsorption constant may be found by:

$$K_{bm} = \frac{nA_{s,0}}{(V_i/V_0)(T - nA_{s,0})} \quad \text{(Eq. 13)}$$

The $A_{s,0}$ is the amount of drug bound to the plasma membrane of a cell at zero time and is determined by extrapolation of a A_c (amount of drug per cell) *versus* t plot to $t = 0$.

The experimental partition coefficient, K_{ex}, is determined from the equilibrium transport conditions; thus:

$$K_{ex} = \frac{C_{c,\infty}}{C_{0,\infty}} = \frac{C_{i,\infty} + K_{bm}C_{0,\infty}}{C_{0,\infty}} \quad \text{(Eq. 14)}$$

whereupon, with Eq. 5:

$$K_{ex} = K + K_{bm} \quad \text{(Eq. 15)}$$

As one observes, the intrinsic partition coefficient K is readily calculated once K_{ex} and K_{bm} are found from the experimental data.

The release transport function, RF_4, is described by:

$$RF_4 = \frac{a(1 + K_{bm}E)}{180G} \ln\left[\frac{GC_c - F}{GC_c(0) - F}\right] = -Pt \quad \text{(Eq. 16)}$$

The model described here for digoxin is not apparently distinguishable from another model (Model 5 in Ref. 2), in which not only the unbound drug but also the external membrane-bound drug permeates across the plasma membrane into the cell. The mathematical expressions, such as Eqs. 9 and 16, are identical in form for both models. Since the authors cannot readily see any accessible experimental means to distinguish Model 5 from this Model 4 and, moreover, believe that the permeability coefficient of the unbound drug is much greater than the permeability coefficient of the membrane-bound drug, Model 4 is considered appropriate for describing the cell transport of digoxin.

Analysis of Results—The profiles of the percent of digoxin taken up by the cells with time in Fig. 5 illustrates several interesting points. The identical uptake profiles of the 5, 15, and 30% fetal bovine serum cases at 33° demonstrate that digoxin does not appreciably bind to the serum. This finding is in agreement with the conclusions of the dialysis experiments. Consistent with the results of the ouabain studies, the uptake rate is faster when there is

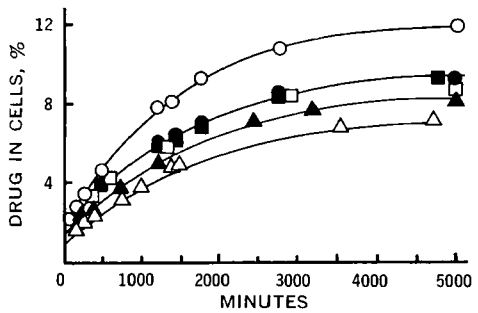

Figure 5—*Uptake rate of digoxin at 26 and 33° by viable Burkitt cells at various fetal bovine serum levels. Solid curves represent the best theoretical fit of the model by nonlinear regression analysis. Key: △, 0% (26°); ▲, 15% (26°); ○, 0% (33°); ●, 5% (33°); □, 15% (33°); and ■, 30% (33°).*

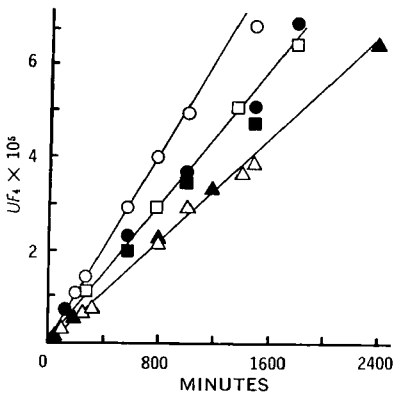

Figure 6—*Profiles of uptake kinetics of digoxin at 26 and 33° and various fetal bovine serum concentrations according to the linear predictions of Eq. 9. Key: △, 0% (26°); ▲, 15% (26°); ○, 0% (33°); ●, 5% (33°); □, 15% (33°); and ■, 30% (33°).*

Table III—Permeability and Partition Coefficients of Digoxin at Various Temperatures and Fetal Bovine Serum Concentrations from Uptake and Release Kinetic Studies[a]

Temperature	Fetal Bovine Serum, %	Intrinsic Partition Coefficient K		Intrinsic Permeability Coefficient P, cm/sec $\times 10^8$	
		Uptake	Release	Uptake	Release
26°	0	11.2 ± 2.1	—	2.93 ± 0.67	—
	15	13.0 ± 2.6	—	2.80 ± 0.56	—
33°	0	17.8 ± 2.7	18.8 ± 2.3	5.01 ± 1.1	3.52 ± 1.8
	5	13.8 ± 2.2	—	3.51 ± 0.71	—
	15	14.7 ± 1.9	17.8 ± 1.7	3.30 ± 0.62	3.75 ± 1.1
	30	12.8 ± 1.3	16.8 ± 1.5	3.21 ± 0.51	3.74 ± 0.8

[a] Values of K and P are average ± SD. The intrinsic partition coefficients were calculated from the equilibrium data according to Eqs. 14 and 15. The intrinsic permeability coefficients were found by nonlinear regression analysis of the model.

no serum present. The uptake rates increase with increasing temperature.

In Fig. 5 there are significant intercepts at zero time, indicative of an initial rapid adsorption of digoxin to the external surface of the plasma membrane. The results of further treatment of these data by the physical model are given in Table II. The plasma membrane–digoxin equilibrium adsorption constant, K_{bm}, is 1.87 at 26° and 1.22 at 33°. These constants are independent of the initial concentration of digoxin used as well as the concentration of fetal bovine serum in the external medium.

In Figs. 6 and 7, the linearity of the curves derived from the treatment of the data for uptake by Eq. 9 and for release by Eq. 16 supports the physical model described in the *Theoretical* section. Examples of the fit of the model to the data by nonlinear regression analysis are shown in Fig. 5.

The intrinsic permeability and partition coefficients from uptake and release studies at 26 and 33° and various fetal bovine serum concentrations are found in Table III. There is a tendency for the intrinsic partition coefficients at 33° to be slightly higher from the release experiments as compared to those from the uptake studies. The reason for this may be attributed to cellular changes occurring over prolonged periods in the release kinetic studies (the total time in loading the cells with digoxin and in the release kinetic portion). However, even when a lower partition coefficient is used along with a permeability coefficient calculated from an uptake experiment, the deviation of the theoretical calculations from the experimental points does not appear to be significant.

Uptake and Release Kinetics of Digitoxin—*Theoretical*—Figure 1 shows the model for the passive transport of unbound digitoxin across the plasma membrane, with rapid distribution within the heterogeneous cell interior as well as the instantaneous reversible linear adsorption of the drug to the external cell surface and the reversible linear binding with the serum in the external media. According to Ref. 2, this system corresponds to the combination of Models 2 and 4.

The mathematical description of this physical model is expressed by the following uptake transport function:

$$UF_{2,4} = -\frac{a[1 + (K_{bm}K_eE/K)]}{180G'} \ln\left[\frac{F - G'C_c}{F - G'C_c(0)}\right] = P_e t \quad \text{(Eq. 17)}$$

$$P_e = \frac{P}{1 + K_b(S)} \quad \text{(Eq. 18)}$$

$$K_e = \frac{K}{1 + K_b(S)} \quad \text{(Eq. 19)}$$

$$E = \frac{nV_i}{V_0} \quad \text{(Eq. 20)}$$

$$F = \left(1 + \frac{K_{bm}}{K}\right)\frac{T}{V_0} \quad \text{(Eq. 21)}$$

$$G' = \left(1 + \frac{K_{bm}}{K}\right)\frac{nV_i}{V_0} + \frac{1}{K_e} \quad \text{(Eq. 22)}$$

where P_e and K_e are the effective permeability and partition coefficients relating to the intrinsic permeability, P, and partition, K, coefficients and serum–drug binding; K_b is the equilibrium serum–drug binding constant; and (S) is the serum concentration in terms of the fraction of the volume of serum added in the total volume of the suspension system.

Before a plot of the uptake function *versus* time in minutes can be made to calculate the intrinsic permeability coefficient in units of centimeters per second from Eq. 17, the constants K, K_b, and K_{bm} must be found. This is readily accomplished by utilizing the data from a family of C_c *versus* t plots at different serum concentrations. The experimental partition coefficient, K_{ex}, is found from the equilibrium situation:

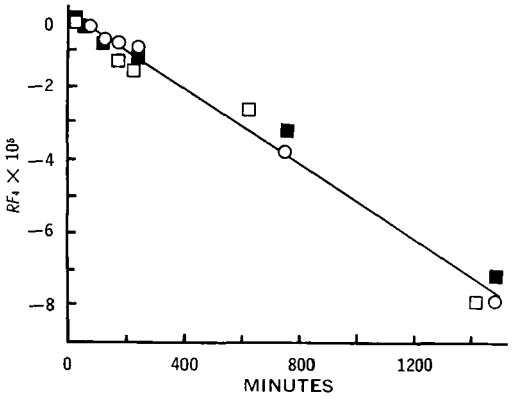

Figure 7—*Profiles of release kinetics of digoxin at 33° and various fetal bovine serum levels according to the linear predictions of Eq. 16. The solid line is derived from least-squares analysis. Key: ○, 0%; □, 15%; and ■, 30%.*

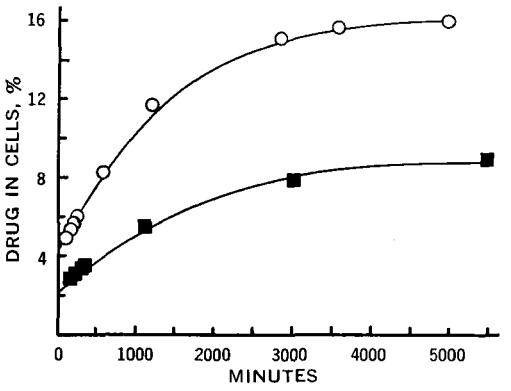

Figure 8—*Uptake rate of digitoxin by viable cells at various fetal bovine serum concentrations at 30°. Solid curves represent the best theoretical fit of the model by nonlinear regression analysis. Key: ○, 0%; and ■, 30%. The positive intercept at initial time is evidence of membrane binding. The lower intercept for the 30% fetal bovine serum case is due to the influence of serum binding and is consistent with the theory (Eqs. 23 and 24).*

Table IV—Effective and Intrinsic Plasma Membrane–Digitoxin Binding Constants at Various Serum Concentrations and Temperatures

Fetal Bovine Serum, %	Effective Membrane Binding Constant[a]			Intrinsic Membrane Binding Constant K_{bm}			Range of Initial Concentration of Digitoxin per 5 ml, dpm
	26°	30°	33°	26°	30°	33°	
0	5.94 ± 0.47	5.81 ± 0.65	5.22 ± 0.67	5.94	5.81	5.22	2×10^5–8.1×10^5
5	—	3.86 ± 0.06	3.90 ± 0.3	—	6.27	6.49	6×10^4–3.5×10^5
15	—	2.76 ± 0.27	2.39 ± 0.09	—	7.94	7.17	8.4×10^4–1.6×10^6
30	2.49 ± 0.31	1.69 ± 0.13	1.96 ± 0.24	—	8.02	9.80	2.5×10^5–8.1×10^5

[a] Values represent the averages ± *SD*. The effective plasma membrane binding constant is defined as $K_{bm}/[1 + K_b(S)]$, where K_{bm} is the intrinsic membrane–drug binding constant, K_b is the serum–drug binding constant, and (S) is the fetal bovine serum concentration. The K_b is 12.5 at 30° and 13.3 at 33°.

Table V—Effective Partition and Permeability Coefficients of Digitoxin at Various Fetal Bovine Serum Concentrations and Temperatures from Uptake Kinetic Studies[a]

Fetal Bovine Serum, %	Effective Partition Coefficients K_e			Effective Permeability Coefficients P_e, cm/sec × 10^8		
	26°	30°	33°	26°	30°	33°
0	28.6 ± 0.9	43.7 ± 3.2	52.0 ± 3.5	10.07 ± 2.48	19.8 ± 1.2	23.0 ± 1.7
5	—	25.0 ± 2.8	35.3 ± 4.9	—	13.0 ± 2.1	15.3 ± 1.1
15	—	14.3 ± 3.2	22.5 ± 2.1	—	6.99 ± 0.88	12.2 ± 3.0
30	10.7 ± 2.1	8.0 ± 1.4	12.0 ± 1.4	2.27 ± 0.33	4.05 ± 0.21	4.91 ± 0.14

[a] All values represent averages ± *SD*. The K_e is obtained from the equilibrium data and the P_e from nonlinear regression analysis of the model; K_e and P_e are defined by Eqs. 18 and 19.

$$K_{ex} = \frac{C_{c,\infty}}{C_{0,\infty}} = \frac{K + K_{bm}}{1 + K_b(S)} \qquad \text{(Eq. 23)}$$

In turn, the membrane–drug binding constant is obtained from the initial condition:

$$K_{bm} = \frac{nA_{s,0}V_0[1 + K_b(S)]}{V_r(T - nA_{s,0})} \qquad \text{(Eq. 24)}$$

The release transport function, $RF_{2,4}$, according to the model is:

$$RF_{2,4} = \frac{a[1 + (K_{bm}K_eE/K)]}{180G'} \ln\left[\frac{G'C_c - F}{G'C_c(0) - F}\right] = -P_e t \qquad \text{(Eq. 25)}$$

Analysis of Results—In Fig. 8, the decrease in the rate of uptake of digitoxin at 30° with increasing concentrations of fetal bovine serum and the percent of the drug associated with the cells at zero time found by extrapolation give evidence that there is binding of the digitoxin not only to the components of the serum but also to the external surface of the plasma membrane[4]. Similar plots are also observed with the uptake experiments at 26 and 33°. The interpretation of serum–digitoxin binding is corroborated by the results of the dialysis experiments described earlier.

The values of the effective equilibrium plasma membrane–digitoxin binding constant at various temperatures and initial concentrations of digitoxin are found in Table IV. The effective membrane–digitoxin binding constant decreases with increasing fetal bovine serum concentrations. The effective membrane binding constant is equal to $K_{bm}/[1 + K_b(S)]$. In Fig. 9, the serum binding constant, K_b, is equal to 12.5 at 30° and 13.3 at 33° and, in turn, the intrinsic membrane binding constant, K_{bm}, can be determined.

It is observed in Table IV that there is no discernible temperature dependence on the K_{bm} at 30 and 33°. Because the calculated K_{bm} is independent of the range of initial concentrations of digitoxin used with respect to a constant concentration of cells, the assumption that the concentration of digitoxin adsorbed is linearly related to the concentration of unbound species in the external fluid is justified. Upon comparing digitoxin with digoxin, the former being more nonpolar than the latter, the propensity of digitoxin to adsorb onto the plasma membrane is about three times greater.

Figure 10 shows the linear relationships of the uptake function of the experimental data at 30° *versus* time at different fetal bovine serum concentrations as predicted by the model. The linear plots of P_{30}/P_e and K_{30}/K_e *versus* percent of fetal bovine serum and the superposition of the points are other indications in support of the model (Fig. 9). The slope is equal to $K_b/(1 + 0.3K_b)$, and the intercept equals $1/(1 + 0.3K_b)$. Accordingly, the K_b is cal-

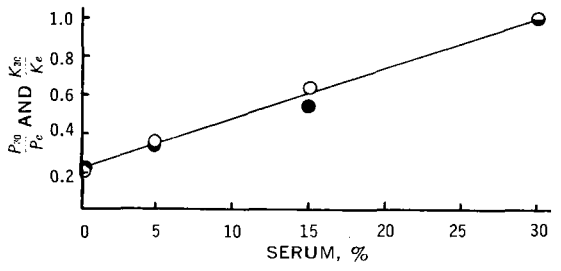

Figure 9—*Normalized plot of the effective permeability and effective partition coefficients of digitoxin as a function of fetal bovine serum concentration. The solid curve represents the least-squares lines. Key:* ●, P_{30}/P_e; *and* ○, K_{30}/K_e.

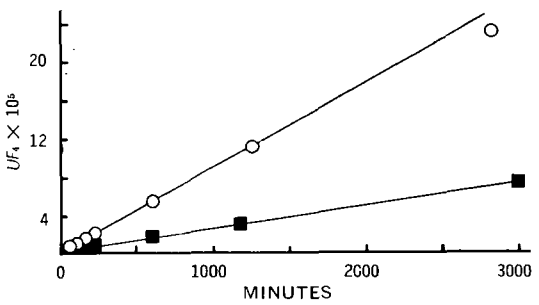

Figure 10—*Profiles of uptake kinetics of digitoxin at 30° according to the linear predictions of Eq. 17. Solid lines are least-squares lines. Key:* ○, *0% fetal bovine serum; and* ■, *30% fetal bovine serum.*

[4] From recent unpublished findings, there appears to be a rapid uptake of digitoxin within the 1st min for which a mechanistic interpretation cannot be made from the kinetic data alone. Taking the uptake and release studies together, it is deemed unlikely that the plasma membrane is not the rate-determining barrier. Autoradiographic studies within this 1-min period are being pursued to examine the distribution of digitoxin on the cell periphery and inside the cell.

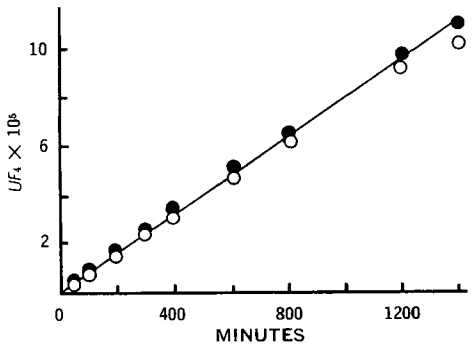

Figure 11—*Uptake kinetics of digitoxin at 30°, showing no effect of antibiotic preservatives in the medium on cell membrane permeability. Key: ●, 15% fetal bovine serum; and ○, 15% fetal bovine serum with penicillin G (50 units/ml) and amphotericin B sulfate (1 μg/100 ml).*

culated to be 12.5, which is equivalent to 92% of the digitoxin being bound reversibly to the fetal bovine serum.

The summary of the phenomenological constants (permeability and partition coefficients) and their relationships to serum levels and temperature are found in Table V.

The addition of penicillin G (50 units/ml) and amphotericin B sulfate (1 μg/100 ml) to the cell suspension to maintain sterility during the transport studies does not seem to have a measurable effect on the uptake kinetics of digitoxin at 30° and 15% fetal bovine serum (Fig. 11). The identical uptake rates by viable and heat-inactivated Burkitt lymphoma cells (Fig. 12) indicate that the transport of digitoxin does not depend upon the viability of the cell and, therefore, is passive.

The change in the concentration of digitoxin in the cell with time in the release kinetic studies and the subsequent data analysis by the release function are shown in Figs. 13 and 14, respectively.

The experimental results of the uptake and release kinetics of digitoxin agree well with the model that accounted for the simultaneous reversible membrane–drug and serum–drug binding across the plasma membrane. This was demonstrated by the linear and nonlinear regression analyses of the data with respect to the physical model. However, additional comments should be made to describe attempts to investigate whether other model variations are also applicable.

The likelihood of irreversible membrane–drug binding, as described by Model 3 (2), is not consistent with the findings that the initial concentration of digitoxin bound to the outer surface of the plasma membrane is proportional to the initial concentration in the external medium (see Table IV). Although the simultaneous passive transport of both the membrane-bound and unbound drug species across the plasma membrane is a possibility, as described by Model 5 (2), this mechanism is deemed less likely on the evidences presented here. Furthermore, if the permeability of the membrane-bound species is smaller than that of the unbound

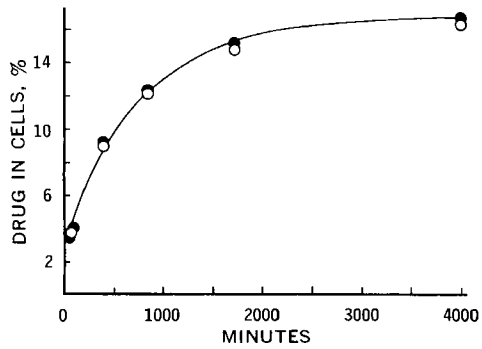

Figure 12—*Uptake of digitoxin with time at 33° and 15% fetal bovine serum. Key: ○, uptake by viable cells; and ●, uptake by heat-inactivated cells. The solid curve is the best-fit curve by nonlinear regression analysis of the model.*

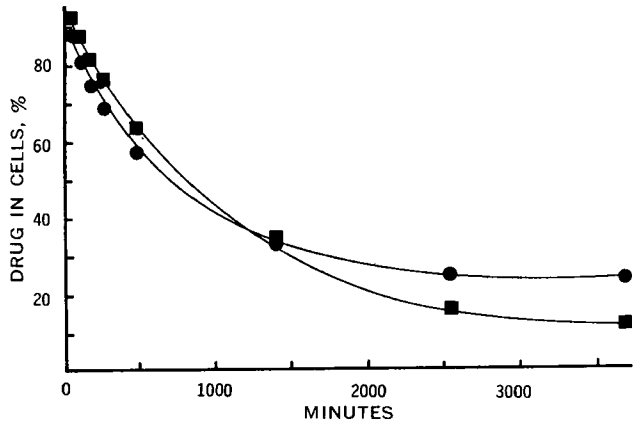

Figure 13—*Release rates of digitoxin from viable cells at 33° into the surrounding medium containing 5% (●) and 30% (■) fetal bovine serum. The cells were initially equilibrated with digitoxin using the static procedure. Solid curves represent the theoretical fit of the model by nonlinear regression analysis.*

species, this model effectively reduces to the model involving the transport of unbound species.

Simultaneous Uptake Kinetics of Ouabain and Digitoxin—*Theoretical*—This model considers the simultaneous uptake of two radiolabeled solutes, such as digitoxin-^{3}H and ouabain-^{3}H, by cells in suspension. It is assumed that both solutes diffuse independently of each other. Let digitoxin be identified as solute *A* and ouabain as solute *B*. As shown previously, digitoxin binds to the plasma membrane and fetal bovine serum while ouabain does not. The cell concentration of both solutes as a function of time is described by the following expression (2):

$$C_{c(A+B)} = (C_{c(A+B),eq} - C_{c,B,eq})e^{-k_B t} + (C_{s,0} - C_{c,A,eq})e^{-k_A t} \quad \text{(Eq. 26)}$$

where:

$$k_A = \frac{3P_{e,A}G'}{a[1 + (K_{bm}K_e E/K)]} \quad \text{(Eq. 27)}$$

$$k_B = \frac{3P_B}{a}\left(\frac{1}{K_B} + \frac{nV_i}{V_0}\right) \quad \text{(Eq. 28)}$$

Analysis of Results—The simultaneous uptake of digitoxin and ouabain at 26° without fetal bovine serum is shown in Fig. 15. Equal concentrations of each cardiac glycoside were added to the cell suspension. The membrane–digitoxin equilibrium constant, K_{bm}, was calculated using the intercept of Fig. 15, the total

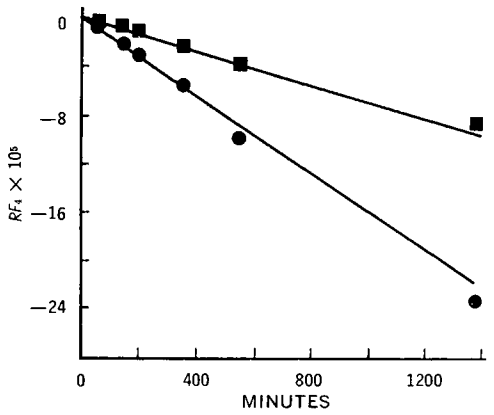

Figure 14—*Profiles of release kinetics of digitoxin at 33° according to the linear predictions of Eq. 25. Solid lines are least-squares lines. Key: ●, 5% fetal bovine serum; and ■, 30% fetal bovine serum.*

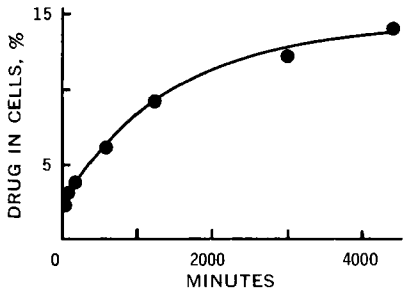

Figure 15—*Simultaneous uptake of digitoxin and ouabain with time by viable cells at 26° in the absence of fetal bovine serum. Experimental points are the sums of both drugs in the cells. The solid curve represents the theoretical predicted curve from the model using the values of the permeability and partition coefficients and other parameters of both drugs from independent experiments. The interpretation is that the transport of digitoxin is independent of that of ouabain and vice versa.*

amount of digitoxin, and the number of cells and was found to be 4.1, which is in reasonable agreement with 5.9 in Table IV. Using the intrinsic partition and permeability coefficients of the glycosides (Tables I and V) and Eq. 26, the theoretical predictions of the $C_{c(A+B)}$ *versus* time plot is in good agreement with the experimental findings. Thus, the passive uptake of digitoxin is not affected by ouabain and vice versa.

DISCUSSION

The kinetic transport data of the cardiac glycosides are consistent with the general physical model involving the rapid equilibration of these solutes within the cell after permeation through the rate-determining plasma membrane barrier. The passive transport of digitoxin is influenced by membrane and serum binding and that of digoxin by membrane binding. There is no binding of ouabain to the plasma membrane and serum.

As reported earlier (3, 4), the sterols (cholesterol, desmosterol, and β-sitosterol) provide complementary examples of the occurrence of only serum binding. In all of these cases the unbound drug molecules appear to be the only kind involved in the penetration of the plasma membrane. Significantly, these studies with the cardiac glycosides and sterols not only provide excellent examples of how each kind of physical interaction, alone and in combination, affect the total transport rate but also demonstrate the method of quantitative factorization of each physical phenomenon and combined interaction from the intrinsic transport rate.

Table VI summarizes the intrinsic phenomenological constants factored out by the analysis of the kinetic data. The intrinsic partition coefficients are direct indications of how much drug actually penetrates the cells. This is an important aspect in the design of drug molecules aside from the interaction of the molecule with the serum and plasma membrane. The intrinsic permeability coefficients indicate the rate at which the drug molecule penetrates the plasma membrane.

Table VI—Summary[a] of Intrinsic Constants of Cardiac Glycosides: Membrane Binding Constant (K_{bm}), Serum Binding Constant (K_b), Partition Coefficient (K), and Permeability Coefficient (P)[a]

Cardiac Glycoside	Temperature	K_{bm}	K_b	K	P, cm/sec × 10^8
Ouabain	26°	0	0	12.2	1.65
	30°	0	0	15.0	2.63
	33°	0	0	15.8	4.51
Digoxin	26°	1.89	0	13.0	2.80
	33°	1.22	0	13.8	3.34
Digitoxin	26°	5.94	—	29.0	10.1
	30°	7.41	12.5	40.0	20.1
	33°	7.82	13.3	59.5	27.4

[a] Values for digitoxin at 26° were taken from uptake studies at 0% fetal bovine serum. All other values were average values from uptake studies only in the presence of fetal bovine serum.

The intrinsic partition and permeability coefficients of ouabain are comparable to those of digoxin, while the coefficients for digitoxin, the most nonpolar among the three cardiac glycosides, are significantly higher. The lack of the hydroxyl group on the 12-position of digoxin giving rise to digitoxin results in significant binding to serum proteins and approximately to a sixfold increase in the membrane binding constant. There is also a threefold increase in the partition coefficient and a 10-fold increase in the permeability coefficient in favor of digitoxin over digoxin with respect to the Burkitt lymphoma cells. Thus, ouabain, digoxin, and digitoxin follow in ascending order of rapidity of their intrinsic transport rates. However, ouabain has the more rapid time for the onset and maximum intensity of cardiac activity *in vivo* following an intravenous digitalizing dose than does digoxin and, in turn, digoxin acts more rapidly than digitoxin (6). Also, the biological half-life is longest with digitoxin, followed by digoxin and then ouabain.

In extrapolating the results of this study with the Burkitt lymphoma cells and fetal bovine serum to the *in vivo* situation, this study supports the hypothesis that the onset and duration of cardiac activity of these glycosides depend upon their relative tendency to bind to serum proteins and nonspecifically to surfaces of cells in the circulatory system because the activity depends upon the availability of unbound drug species for transport across the membranes of capillaries and heart muscle cells. The intrinsic uptake and release kinetics and membrane binding of the glycosides by nonheart muscle cells and tissues will affect the biological half-life. The enterohepatic cycling of digoxin and digitoxin and the biotransformation of digitoxin are other influential, kinetically dimensional factors (7).

In the specific case of digoxin, the rate-determining step for the onset of cardiac activity may be the transport of the unbound digoxin across the capillary membrane and not across the membrane of the heart muscle cell, since the pharmacological action seems to be focused upon a surface interaction on the cell membrane. This is indicated by a recent study (8) correlating the inotropic and chronotropic activities of isolated beating neonatal rat heart cells in a culture system with membrane-bound digoxin[5].

In Figs. 3, 6, 10, 11, and 14, it is sometimes observed that the scatter of the data about the linear regression line increases as the transport of the drug proceeds to equilibrium. This is largely due to the logarithmic nature of the uptake concentration function; a small experimental error in the assay of the drug in the cells leads to a more pronounced deviation in these plots near equilibrium. At equilibrium the function equals zero and is, therefore, undefined. The deviation encountered when linear regression analysis is used disappears when the nonlinear regression technique is employed.

The experimental techniques used here are satisfactory for drugs with low permeability coefficients (5×10^{-5} and smaller) and with relatively high partition coefficients (at least 5) because the sampling time is of the order of 3 min and the centrifugation step takes 10 min. Another limitation is the low partition coefficient, which leads to analytical problems. Circumvention of this analytical constraint might be possible by increasing the cell volume fraction.

The combined usage of the mathematical models and experimental methodology developed along the guidelines of the models demonstrate the advantages of the physical model approach to the quantitative analysis of experimental data to yield meaningful phenomenological parameters. The far-reaching goal of this approach is to predict drug activity *in vivo*. This work should be regarded as a useful tool for the examination of many cells and tissues and their relationship to drugs that affect them. This system provides an excellent method for quantifying cellular drug availability as a function of molecular design. It is not intended to preclude other distribution and metabolic factors operative in the whole animal.

REFERENCES

(1) N. F. H. Ho, J. S. Turi, C. Shipman, Jr., and W. I. Higuchi,

[5] According to the calculations of the uptake studies of digoxin with neonatal rat heart cells at 37°, K_b is negligible, $K_{bm} = 34$, $K = 187$, and $P = 1.6 \times 10^{-5}$ cm/sec.

J. Theoret. Biol., **34**, 451(1972).
(2) J. S. Turi, N. F. H. Ho, W. I. Higuchi, and C. Shipman, Jr., *J. Pharm. Sci.*, **64**, 622(1975).
(3) J. S. Turi, W. I. Higuchi, C. Shipman, Jr., and N. F. H. Ho, *ibid.*, **61**, 1618(1972).
(4) J. S. Turi, W. I. Higuchi, N. F. H. Ho, and C. Shipman, Jr., *ibid.*, **64**, 627(1975).
(5) J. E. Doherty and W. H. Hall, *Amer. J. Cardiol.*, **28**, 326(1971).
(6) "The Pharmacological Basis of Therapeutics," 4th ed., L. S. Goodman and A. Gilman, Eds., Macmillan, New York, N.Y., 1970, p. 699.
(7) G. T. Okita, *Fed. Proc.*, **26**, 1125(1967).
(8) T. B. Okarma, P. Trammell, and S. M. Kalman, *J. Pharmacol. Exp. Ther.*, **183**, 559(1972).

ACKNOWLEDGMENTS AND ADDRESSES

Received February 13, 1974, from **Pharmacy Research, The Upjohn Company, Kalamazoo, MI 49001*, the *‡College of Pharmacy, University of Michigan, Ann Arbor, MI 48104*, and the *§Dental Research Institute, Department of Oral Biology, School of Dentistry, and the Department of Microbiology, School of Medicine, University of Michigan, Ann Arbor, MI 48104*

Accepted for publication July 19, 1974.

ˣ To whom inquiries should be directed.

Antiarrhythmic Activity of 3-Amino-3-methyloxindoles

M. J. KORNET ˣ, P. A. THIO, N. MALONE, and W. C. LUBAWY

Abstract □ A series of 3-amino-3-methyloxindoles was synthesized from indoles by modification of previously described procedures. All compounds showed activity against chloroform-induced arrhythmias in mice. One member of the series, 3-methyl-3-piperidinooxindole, displayed activity equal to that of lidocaine while showing only one-third the acute toxicity.

Keyphrases □ 3-Amino-3-methyloxindoles—synthesis, antiarrhythmic activity, compared to lidocaine □ Antiarrhythmic activity—3-amino-3-methyloxindoles synthesized and screened

The authors' interest in the synthesis and pharmacological evaluation of lidocaine (I) analogs goes back several years, and initially attention was focused on compounds where the basic group was a hydrazine derivative (1). Recent work in these laboratories on the chemistry of aminooxindoles (2) has led to an expansion of this interest and to the present report concerning the synthesis and antiarrhythmic activity of a series of 3-amino-3-methyloxindoles (II).

Examination of II showed that these compounds incorporate the principal structural moieties of the local anesthetic and antiarrhythmic drug lidocaine—*viz.*, an aromatic nucleus, an amide linkage, and a basic amino group, in a nearly rigid framework. Closer examination revealed that the title compounds possess unique structural features that set them apart from lidocaine and its many congeners. Significant differences can be discerned in the stereochemistry of II and lidocaine. Thus, II has the *cis*-amide configuration, while the protonated form of lidocaine, which is supposed to be the active form of the drug, has the *trans*-configuration (3). Another difference is found in the coplanarity of the amide carbonyl group with respect to the aromatic moiety; steric hindrance precludes such a conformation in the lidocaine molecule (3, 4). Finally, it is worth noting that in II, in contrast to lidocaine, the "activity-controlling distance" (5) between the basic nitrogen and the amide carbonyl and aromatic nucleus is completely fixed.

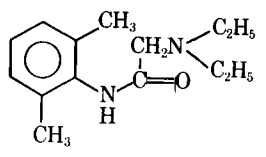

I

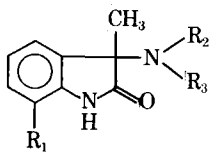

II

Because of its flexible structure, lidocaine can acquire a large variety of conformations and may, therefore, possibly fit a number of different receptor sites (6, 7). On the other hand, if a rigid congener of lidocaine can be found of the proper stereochemical configuration and charge distribution to give a high degree of complementariness to the receptor responsible for antiarrhythmic action, this hypothetical compound should show a more highly specific interaction (8). Since a full coincidence of stereochemical properties for the different receptors involved in the action of a multipotent drug is rather unlikely, this specificity should help to minimize side effects that originate from interaction with other receptor types as well as those that result from degradation of the drug into biologically active metabolites (9). In addition, such a hypothetical compound may be presumed to be highly active (7) and hence efficacious in smaller doses; this, in turn, should lower any associated "physical toxicity" (8) due to nonspecific drug action (10).

RESULTS AND DISCUSSION

The title compounds were obtained from indoles by modification of the procedures described by Hinman and Bauman (11, 12) (Scheme I). They prepared 3-bromo-3-methyloxindole by the *N*-bromosuccinimide bromination–oxidation of skatole (11); but in repeating this work, considerable difficulty was experienced in